Preparation and Characterization of Palladium(I) and Platinum(I) Dinuclear Complexes Bridged by 2-(Dimethylphosphino)pyridine

Takayoshi SUZUKI and Junnosuke FUJITA*
Department of Chemistry, Faculty of Science, Nagoya University,
Furo-cho, Chikusa-ku, Nagoya 464-01
(Received November 8, 1991)

A series of dinuclear complexes containing Me_2Ppy (=2-(dimethylphosphino)pyridine) as a bridging ligand, $[MM'X_2(\mu\text{-}Me_2Ppy)_2]$ (M, M'=Pd(I), Pt(I); X=Cl, Br, and I), have been prepared by reactions between $[MX_2(Me_2Ppy\text{-}P)_2]$ and $[M'_2(dba)_3]$ (dba=1,5-diphenyl-1,4-pentadien-3-one). In these reactions it has been found by $^{31}P\{^1H\}$ NMR studies that a dimeric head-to-head isomer was formed in the first place and then isomerized to a head-to-tail isomer. The reactions for analogous Ph_2Ppy (=2-(diphenylphosphino)pyridine) complexes have been also examined in the same manner. The monomeric Pd(II) complexes reacted more rapidly than did the corresponding Pt(II) complexes in these dimerization and isomerization reactions. For each halogeno series of the Me_2Ppy and Ph_2Ppy complexes, it seems that the dimerization occurs faster in the order of Cl<Br<I, while the order is reversed in the isomerization, Cl>Br>I. The Me_2Ppy complexes isomerized to a head-to-tail isomer more rapidly than did the Ph_2Ppy complexes, indicating a larger trans effect of Me_2Ppy than Ph_2Ppy.

A large number of Pd(I) and Pt(I) complexes involving a metal–metal bond and a bridging bidentate ligand have been prepared by a conproportionation reaction between appropriate complexes of M(II) and M(O) (M=Pd, Pt).[1-8] When the bidentate ligand is unsymmetrical, the dinuclear complex has two possible geometrical isomers, head-to-head (*HH*) and head-to-tail (*HT*) (Fig. 1). For $[Pt_2I_2(\mu\text{-}Ph_2Ppy)_2]$ (Ph_2Ppy=2-(diphenylphosphino)pyridine), these two isomers were obtained by Farr, Wood, and Balch.[7] In a previous paper,[9] we have reported the preparation and characterization of mononuclear Pd(II) and Pt(II) complexes containing unidentate phosphorus donating or chelating 2-(dimethylphosphino)pyridine (=Me_2Ppy). The Me_2Ppy ligand is less bulky and more basic than Ph_2Ppy, and hence would have a stronger affinity to a metal ion. However, $[AuX(Me_2Ppy\text{-}P)]$ and $[Au_2(\mu\text{-}Me_2Ppy)_2]^{2+}$, in which no metal–metal bond is involved, are only known Me_2Ppy complexes to our knowledge.[10] This paper deals with the preparation and characterization of dinuclear Pd(I) and Pt(I) complexes containing Me_2Ppy as a bridging ligand. Comparisons of reaction profiles in dimeric complex formation between the Me_2Ppy and Ph_2Ppy complexes are also described.

Experimental

Me_2Ppy, $[PdX_2(Me_2Ppy\text{-}P)_2]$, $[PtX_2(Me_2Ppy\text{-}P)_2]$, and $[PdX_2(Ph_2Ppy\text{-}P)_2]$ (X=Cl, Br, and I) were prepared as described previously.[9] $[PtX_2(Ph_2Ppy\text{-}P)_2]$ (X=Cl, Br,[11] and I[7]) and $[M_2(dba)_3]\cdot CHCl_3$ (M=Pd[12] and Pt[13]; dba=1,5-diphenyl-1,4-pentadien-3-one) were obtained according to the literature methods.

Preparation of Dinuclear Complexes. *HT*-$[Pd_2Cl_2(\mu\text{-}Me_2Ppy)_2]$: A mixture of $[PdCl_2(Me_2Ppy\text{-}P)_2]$ (456 mg, 1.00 mmol) and $[Pd_2(dba)_3]\cdot CHCl_3$ (514 mg, 0.50 mmol) in dichloromethane (50 cm^3) was refluxed at 40 °C under a nitrogen atmosphere with stirring for 10 h. The mixture was then filtered in air to remove a trace amount of a black precipitate, and the filtrate was evaporated to ca. 5 cm^3 under reduced pressure. Diethyl ether (ca. 100 cm^3) was added with vigorous stirring, and the resulting precipitate was collected by filtration, washed with diethyl ether (ca. 30 cm^3), and dried in air.

The crude product was dissolved in hot ethanol (60—70 °C), and the solution was filtered while in hot. The filtrate was slowly cooled to 0 °C to yield fine-shaped crystals, which were collected by filtration and dried in air.

The yields, crystal colors and habits, and analytical data for the complexes prepared in this study are given in Table 1.

***HT*-$[Pd_2Br_2(\mu\text{-}Me_2Ppy)_2]$ and *HT*-$[Pd_2I_2(\mu\text{-}Me_2Ppy)_2]\cdot 1/2CH_2Cl_2$:** The crude products of these complexes were obtained similarly by heating $[PdBr_2(Me_2Ppy\text{-}P)_2]$ or $[PdI_2(Me_2Ppy\text{-}P)_2]$ with $[Pd_2(dba)_3]\cdot CHCl_3$ in dichloromethane for 4 h.

The red precipitate of the bromo complex was dissolved in hot methanol (50—60 °C), and the solution was filtered while in hot. The filtrate was cooled slowly to room temperature, and then stored in a refrigerator over night to yield fine-shaped crystals, which were collected by filtration and dried in air.

The red precipitate of the iodo complex was recrystallized from a mixture of dichloromethane and methanol (2:1). Slow evaporation of the solvent in a desiccator yielded fine-shaped crystals, which were collected by filtration and dried in air.

***HT*-$[Pt_2Cl_2(\mu\text{-}Me_2Ppy)_2]$ and *HT*-$[Pt_2Br_2(\mu\text{-}Me_2Ppy)_2]$:** These complexes were prepared by a method similar to that for the dipalladium complex, from $[PtX_2(Me_2Ppy\text{-}P)_2]$ (X=Cl and Br, 1.00 mmol) and $[Pt_2(dba)_3]\cdot CHCl_3$ (0.50 mmol). Heating was continued for 5 d for the chloro complex, and 3 d for the bromo complex. The crude products of the chloro and bromo complexes were recrystallized from hot ethanol and hot methanol, respectively.

***HT*-$[Pt_2I_2(\mu\text{-}Me_2Ppy)_2]\cdot 1/2CH_2Cl_2$:** A red brown precipitate was obtained similarly by reaction of $[PtI_2(Me_2Ppy\text{-}P)_2]$ with $[Pt_2(dba)_3]\cdot CHCl_3$ for 3 d, and by addition of diethyl ether. The precipitate was shown by the $^{31}P\{^1H\}$ NMR spectrum to be a 2:1 mixture of the *HT*- and *HH*-isomers. The *HT*-isomer was obtained by repeated recrystallization from a mixture of dichloromethane and methanol (2:1) according to the same method as for *HT*-$[Pd_2I_2(\mu\text{-}Me_2Ppy)_2]$, but isolation of the pure *HH*-isomer was unsuccessful.

***HT*-[PdPtCl$_2$(μ-Me$_2$Ppy)$_2$]:** A dichloromethane solution containing [PtCl$_2$(Me$_2$Ppy-*P*)$_2$] (1.00 mmol) and [Pd$_2$(dba)$_3$]·CHCl$_3$ (0.50 mmol) was heated for 24 h under a nitrogen atmosphere. The mixture was filtered in air, and the filtrate was evaporated to ca. 5 cm^3 under reduced pressure. On addition of diethyl ether the solution gave an orange precipitate. It was dissolved in hot ethanol, and the solution was cooled slowly to yield red prismatic crystals of the desired complex together with yellow thin plate crystals of unreacted *cis*-[PtCl$_2$(Me$_2$Ppy-*P*)$_2$]. These crystals were separated by hand-picking under a microscope, and the red crystals were recrystallized again from hot ethanol.

***HT*-[PdPtBr$_2$(μ-Me$_2$Ppy)$_2$]:** A mixture of this complex and the unreacted Pt(II) complex was obtained from [PtBr$_2$(Me$_2$Ppy-*P*)$_2$] and [Pd$_2$(dba)$_3$]·CHCl$_3$ by the same method as the above, except that the reaction time was 10 h. Recrystallization from hot methanol, separation of two kinds of crystals by hand-picking, and further recrystallization from hot methanol gave red crystals of the complex.

***HT*-[PdPtI$_2$(μ-Me$_2$Ppy)$_2$]·1/2CH$_2$Cl$_2$:** The complex was prepared similarly by reaction of [PtI$_2$(Me$_2$Ppy-*P*)$_2$] and [Pd$_2$(dba)$_3$]·CHCl$_3$ for 10 h. The crude product was recrystallized by dissolving in a mixture of dichloromethane and methanol (2 : 1) and by evaporating the solvent slowly at 0 °C, yielding red-brown crystals of the complex.

***HT*-[Pd$_2$X$_2$(μ-Ph$_2$Ppy)$_2$]·1/2CH$_2$Cl$_2$ (X=Cl, Br, and I):** These complexes were prepared by a similar method for *HT*-[Pd$_2$Cl$_2$(μ-Ph$_2$Ppy)$_2$].[14] The reaction time for the chloro complex was 24 h, and those for the bromo and iodo complexes were 16 h. The crude products obtained by addition of diethyl ether were recrystallized from a mixture of dichloromethane and methanol (2 : 1) by a method similar to that for *HT*-[Pd$_2$I$_2$(μ-Me$_2$Ppy)$_2$].

***HT*-[Pt$_2$Cl$_2$(μ-Ph$_2$Ppy)$_2$]·1/2CH$_2$Cl$_2$:** This complex was prepared by a literature method.[7] The crude product was recrystallized from a mixture of dichloromethane and methanol (2 : 1) to form fine-shaped crystals.

***HH*-[Pt$_2$Br$_2$(μ-Ph$_2$Ppy)$_2$] and *HT*-[Pt$_2$Br$_2$(μ-Ph$_2$Ppy)$_2$]·1/2CH$_2$Cl$_2$:** The reaction of [PtBr$_2$(Ph$_2$Ppy-*P*)$_2$] (881 mg, 1.00 mmol) with [Pt$_2$(dba)$_3$]·CHCl$_3$ (616 mg, 0.50 mmol) in dichloromethane for 3 d, followed by addition of diethyl ether yielded an orange precipitate. It was collected by filtration, dried in air, mixed with ca. 5 cm^3 of dichloromethane at ambient temperature, and an undissolved yellow precipitate was removed by immediate filtration.

On the red filtrate methanol (ca. 20 cm^3) was layered, and the mixture was allowed to stand to form red crystals of *HT*-[Pt$_2$Br$_2$(μ-Ph$_2$Ppy)$_2$], which were collected by filtration and recrystallized repeatedly from dichloromethane and methanol.

The yellow precipitate which had remained undissolved was dissolved in ca. 30 cm^3 of dichloromethane, and filtered. On the filtrate ca. 50 cm^3 of methanol was layered, and the mixture was allowed to stand. Orange-yellow crystals of *HH*-[Pt$_2$Br$_2$(μ-Ph$_2$Ppy)$_2$] formed were collected by filtration and dried in air.

***HT*-[Pt$_2$I$_2$(μ-Ph$_2$Ppy)$_2$]·1/2CH$_2$Cl$_2$:** The literature method[7] was modified for the preparation of this complex. To a dichloromethane solution (10 cm^3) of *HT*-[Pt$_2$Cl$_2$(μ-Ph$_2$Ppy)$_2$]·1/2CH$_2$Cl$_2$ (100 mg, 0.097 mmol) was added a methanol solution (25 cm^3) of KI (100 mg, 0.60 mmol). After stirring over night the mixture was evaporated to dryness under reduced pressure, and the residue was extracted with dichloromethane (ca. 30 cm^3). The volume of the extract was reduced to ca. 5 cm^3 by evaporation, and methanol (10 cm^3) was added. The mixture was allowed to stand in a refrigerator over night to form purple-red crystals, which were collected by filtration and dried in air. Yield 70 mg (58%).

***HH*-[Pt$_2$I$_2$(μ-Ph$_2$Ppy)$_2$]:** The complex was prepared by the literature method.[7] The fine-shaped crystals were obtained by layering methanol on a dichloromethane solution of the complex in a similar manner to that for *HH*-[Pt$_2$Br$_2$(μ-Ph$_2$Ppy)$_2$].

***HT*-[PdPtX$_2$(μ-Ph$_2$Ppy)$_2$]·1/2CH$_2$Cl$_2$ (X=Cl, Br, and I):** These complexes were prepared by the literature methods.[7] The pure and fine-shaped crystals were obtained by recrystallization from a mixture of dichloromethane and methanol (1 : 1).

Measurements. Infrared spectra in the range 700—200 cm^{-1} were obtained with a Hitachi EPI-L spectrometer by the Nujol mull method using polyethylene films. ^{1}H, ^{13}C{^{1}H}, ^{31}P{^{1}H} NMR spectra of CDCl$_3$ solutions were recorded at 90.02, 22.66, and 36.46 MHz, respectively, on a Hitachi R-90HS spectrometer at 33 °C. Tetramethylsilane was used as an internal reference for ^{1}H and ^{13}C{^{1}H} NMR spectra, and 85% H$_3$PO$_4$ was used as an external reference for ^{31}P{^{1}H} NMR spectra. UV-visible spectra of dichloromethane solutions were measured at 24 °C on a Hitachi U-3410 spectrophotometer.

Results and Discussion

Preparation and Characterization of Dinuclear Complexes. The dinuclear Pd(I) and Pt(I) complexes bridged by Me$_2$Ppy were prepared by a conproportionation reaction (1) reported for the Ph$_2$Ppy complexes.[6,7]

$$[MX_2(R_2Ppy\text{-}P)_2] + 1/2\,[M'_2(dba)_3] \rightarrow [MM'X_2(\mu\text{-}R_2Ppy)_2]$$
(M, M'=Pd, Pt; X=Cl, Br, I; R=Me, and Ph) (1)

All of the Me$_2$Ppy complexes obtained by reaction (1) have the composition of [MM'X$_2$(R$_2$Ppy)$_2$], and are a non-electrolyte as shown by elemental analyses and conductivity measurements, respectively (Table 1). In the infrared spectra, the complexes show a band due to the in-plane ring deformation of pyridyl moiety around 645—650 cm^{-1}, indicating the nitrogen atom being bound to the metal ion.[9] The unidentate phosphorus donating R$_2$Ppy in Pd(II) and Pt(II) complexes exhibits the band around 615—620 cm^{-1}.[9] Thus the complexes

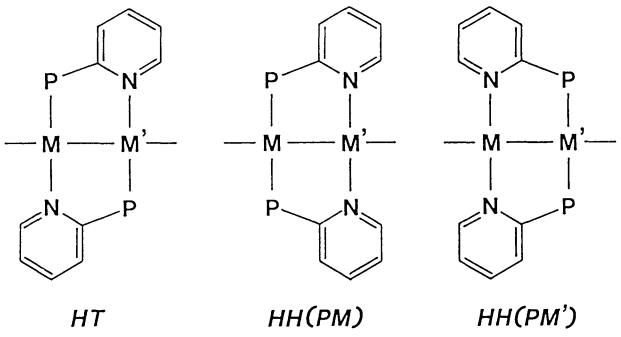

Fig. 1. Geometrical isomers of [MM'X$_2$(μ-R$_2$Ppy)$_2$]; head-to-tail (*HT*) and head-to-head (*HH*).

will have the same dinuclear structure as that of the Ph_2Ppy complexes, and can exist in the head-to-head (*HH*) and the head-to-tail (*HT*) isomers. For a heterodinuclear complex, there are two possible *HH*-isomers, *HH*(*PPd*) and *HH*(*PPt*) (Fig. 1).

Farr, Wood, and Balch[7] assigned geometrical structures of the dinuclear Pt(I)–Pt(I) and Pd(I)–Pt(I) complexes of Ph_2Ppy on the basis of characteristic $^{31}P\{^1H\}$

Table 1. Yields, Crystal Colors and Habits, and Analytical Data of the Dinuclear Complexes

Complex	Yield	Crystal		Found (Calcd)		
	%	Color	Habit	C/%	H/%	N/%
HT-[$Pd_2Cl_2(\mu$-$Me_2Ppy)_2$]	87.4	Dark red	Prism	30.06(29.92)	3.70(3.59)	5.02(4.98)
HT-[$Pd_2Br_2(\mu$-$Me_2Ppy)_2$]	86.2	Red	Needle	25.97(25.83)	2.97(3.10)	4.37(4.30)
HT-[$Pd_2I_2(\mu$-$Me_2Ppy)_2$]·1/2CH_2Cl_2	80.8	Dark red	Prism	25.57(22.12)	2.78(2.69)	3.53(3.56)
HT-[$Pt_2Cl_2(\mu$-$Me_2Ppy)_2$]	67.5	Yellow-orange	Prism	22.57(22.74)	2.98(2.73)	3.71(3.79)
HT-[$Pt_2Br_2(\mu$-$Me_2Ppy)_2$]	65.1	Red-orange	Needle	20.76(20.30)	2.52(2.43)	3.15(3.38)
HT-[$Pt_2I_2(\mu$-$Me_2Ppy)_2$]·1/2CH_2Cl_2	25.9	Red-brown	Prism	18.57(18.05)	1.96(2.19)	2.75(2.90)
HT-[$PdPtCl_2(\mu$-$Me_2Ppy)_2$]	37.5	Red	Prism	26.06(25.84)	3.19(3.10)	4.27(4.31)
HT-[$PdPtBr_2(\mu$-$Me_2Ppy)_2$]	62.4	Red	Needle	22.75(22.74)	2.77(2.73)	3.79(3.79)
HT-[$PdPtI_2(\mu$-$Me_2Ppy)_2$]·1/2CH_2Cl_2	54.8	Red-brown	Prism	19.33(19.88)	2.15(2.42)	2.91(3.20)
HT-[$Pd_2Cl_2(\mu$-$Ph_2Ppy)_2$]·1/2CH_2Cl_2[a]	66.2	Dark red	Prism	47.67(48.59)	3.07(3.43)	3.15(3.29)
HT-[$Pd_2Br_2(\mu$-$Ph_2Ppy)_2$]·1/2CH_2Cl_2	90.0	Dark red	Needle	43.68(44.00)	2.94(3.10)	2.99(2.97)
HT-[$Pd_2I_2(\mu$-$Ph_2Ppy)_2$]·1/2CH_2Cl_2	85.3	Dark purple	Needle	38.28(40.01)	2.52(2.82)	2.67(2.70)
HT-[$Pt_2Cl_2(\mu$-$Ph_2Ppy)_2$]·1/2CH_2Cl_2[b]	19.5	Red	Prism	40.66(40.23)	2.64(2.84)	2.72(2.72)
HT-[$Pt_2Br_2(\mu$-$Ph_2Ppy)_2$]·1/2CH_2Cl_2	11.9	Red	Prism	37.40(37.03)	2.42(2.61)	2.35(2.50)
HH-[$Pt_2Br_2(\mu$-$Ph_2Ppy)_2$]	10.0	Orange	Prism	38.09(37.93)	2.43(2.61)	2.44(2.60)
HH-[$Pt_2I_2(\mu$-$Ph_2Ppy)_2$][b]	34.8	Orange	Prism	35.05(34.89)	2.17(2.41)	2.28(2.39)
HT-[$Pt_2I_2(\mu$-$Ph_2Ppy)_2$]·1/2CH_2Cl_2[b]	58	Red-purple	Needle	34.31(34.16)	2.25(2.41)	2.28(2.31)
HT-[$PdPtCl_2(\mu$-$Ph_2Ppy)_2$]·1/2CH_2Cl_2[b]	68.2	Red	Prism	44.08(44.02)	2.94(3.10)	2.87(2.98)
HT-[$PdPtBr_2(\mu$-$Ph_2Ppy)_2$]·1/2CH_2Cl_2	62.6	Red	Prism	39.51(40.22)	2.61(2.84)	2.61(2.72)
HT-[$PdPtI_2(\mu$-$Ph_2Ppy)_2$]·1/2CH_2Cl_2[b]	65.3	Dark red	Prism	36.65(36.86)	2.38(2.60)	2.36(2.49)

a) Ref. 14. b) Ref. 7.

Table 2. $^{31}P\{^1H\}$ NMR Data of the Dinuclear Complexes[a]

Complex	δ(P-Pd)	δ(P-Pt)	$^1J_{P\text{-}Pt}$	$^2J_{P\text{-}Pt}$	$^3J_{P\text{-}P}$
HT-[$Pd_2Cl_2(\mu$-$Me_2Ppy)_2$]	−23.56				
HT-[$Pd_2Br_2(\mu$-$Me_2Ppy)_2$]	−25.83				
HT-[$Pd_2I_2(\mu$-$Me_2Ppy)_2$]	−30.17				
HH-[$Pd_2Cl_2(\mu$-$Me_2Ppy)_2$][b]	−33.17				
HH-[$Pd_2Br_2(\mu$-$Me_2Ppy)_2$][b]	−36.29				
HH-[$Pd_2I_2(\mu$-$Me_2Ppy)_2$][b]	−41.73				
HT-[$Pt_2Cl_2(\mu$-$Me_2Ppy)_2$]		−31.78	3985	213.5	18.9
HT-[$Pt_2Br_2(\mu$-$Me_2Ppy)_2$]		−34.13	3919	212.4	18.9
HT-[$Pt_2I_2(\mu$-$Me_2Ppy)_2$]		−38.00	3827	199.1	18.9
HH-[$Pt_2I_2(\mu$-$Me_2Ppy)_2$][b]		−16.84	2957	131.2	
HT-[$PdPtCl_2(\mu$-$Me_2Ppy)_2$]	−20.98	−37.16	3910	90.1	14.5
HT-[$PdPtBr_2(\mu$-$Me_2Ppy)_2$]	−22.88	−39.34	3849	71.2	15.6
HT-[$PdPtI_2(\mu$-$Me_2Ppy)_2$]	−26.79	−42.96	3764	37.8	16.7
HH-[$PdPtI_2(\mu$-$Me_2Ppy)_2$][b]		−27.08	2912		
HT-[$Pd_2Cl_2(\mu$-$Ph_2Ppy)_2$]	3.72				
HT-[$Pd_2Br_2(\mu$-$Ph_2Ppy)_2$]	2.31				
HT-[$Pd_2I_2(\mu$-$Ph_2Ppy)_2$]	0.37				
HH-[$Pd_2Cl_2(\mu$-$Ph_2Ppy)_2$][b]	−12.38				
HH-[$Pd_2Br_2(\mu$-$Ph_2Ppy)_2$][b]	−14.31				
HH-[$Pd_2I_2(\mu$-$Ph_2Ppy)_2$][b]	−16.6				
HT-[$Pt_2Cl_2(\mu$-$Ph_2Ppy)_2$]		−2.29	4128	215.7	17.8
HT-[$Pt_2Br_2(\mu$-$Ph_2Ppy)_2$]		−3.75	4048	213.5	17.8
HT-[$Pt_2I_2(\mu$-$Ph_2Ppy)_2$]		−6.25	3965	204.6	20.0
HH-[$Pt_2Cl_2(\mu$-$Ph_2Ppy)_2$][b]		14.64			
HH-[$Pt_2Br_2(\mu$-$Ph_2Ppy)_2$]		12.17	3589	160.1	
HH-[$Pt_2I_2(\mu$-$Ph_2Ppy)_2$]		9.34	3263	153.5	
HT-[$PdPtCl_2(\mu$-$Ph_2Ppy)_2$]	7.06	−7.52	4049	105.7	14.5
HT-[$PdPtBr_2(\mu$-$Ph_2Ppy)_2$]	5.89	−8.89	3978	91.2	15.6
HT-[$PdPtI_2(\mu$-$Ph_2Ppy)_2$]	3.46	−10.93	3894	64.5	16.1

a) Chemical shifts are relative to 85% H_3PO_4 in the δ-scale, and coupling constants are in Hz.
b) These complexes are only detected spectroscopically.

and $^{195}Pt\{^1H\}$ NMR spectra arising from the one- and two-bond Pt–P, and $^3J_{(P,P)}$ coupling constants. The structures of dinuclear Pt(I) complexes of Me_2Ppy and new dibromo Pt(I) complexes of Ph_2Ppy were assigned similarly from studies of the $^{31}P\{^1H\}$ NMR spectra. The results are given in Table 2 along with the spectral data, and Fig. 2 shows the $^{31}P\{^1H\}$ NMR spectra of *HT*-$[Pt_2Cl_2(\mu\text{-}Me_2Ppy)_2]$, *HT*-$[PdPtCl_2(\mu\text{-}Me_2Ppy)_2]$, and *HH*-$[Pt_2Br_2(\mu\text{-}Ph_2Ppy)_2]$. For the structure assignment of Pd–Pd complexes, $^{31}P\{^1H\}$ NMR spectroscopy is not effective. The spectra exhibit only one singlet peak. However, the structures of Me_2Ppy complexes can be assigned on the basis of the spectral pattern of P–CH_3 in $^{13}C\{^1H\}$ and ^1H NMR (Table 3). Figure 3 shows ^1H and $^{13}C\{^1H\}$ NMR spectra of the P–CH_3 in *HT*-$[Pd_2Br_2(\mu\text{-}Me_2Ppy)_2]$. These spectral patterns can only be understood by considering the phosphorus–phosphorus coupling as well as the phosphorus–proton or phosphorus–carbon one. The $J_{(P,P)}$ values evaluated from spectral simulation is small, ca. 15 Hz. This small value would correspond to the one for a three-bond P–P coupling, $^3J_{(P,P)}$ in the *HT* structure. Similar $^3J_{(P,P)}$ values are obtained directly from the $^{31}P\{^1H\}$ NMR spectra of *HT*-isomers of the Pt(I) complexes (Table 2). A *HH*-isomer would have a much larger $^2J_{(P,P)}$ value as reported for $[Pd_2Cl_2(\mu\text{-dppm})(\mu\text{-Medppm})]$ (ca. 440 Hz), where dppm and Medppm denote $(C_6H_5)_2PCH_2P(C_6H_5)_2$ and $(C_6H_5)_2PCH(CH_3)P(C_6H_5)_2$, respec-

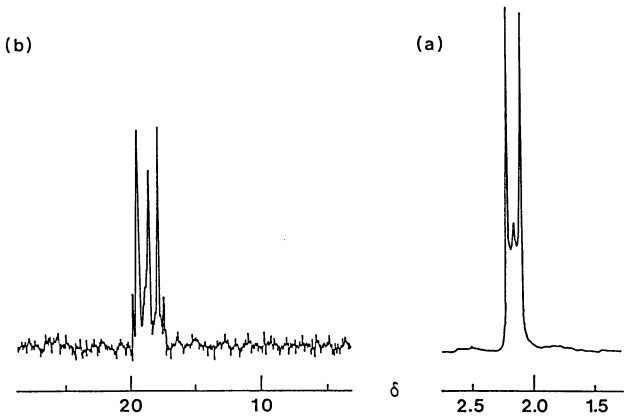

Fig. 3. ^1H (a) and $^{13}C\{^1H\}$ (b) NMR spectra of the P–CH_3 in *HT*-$[Pd_2Br_2(\mu\text{-}Me_2Ppy)_2]$.

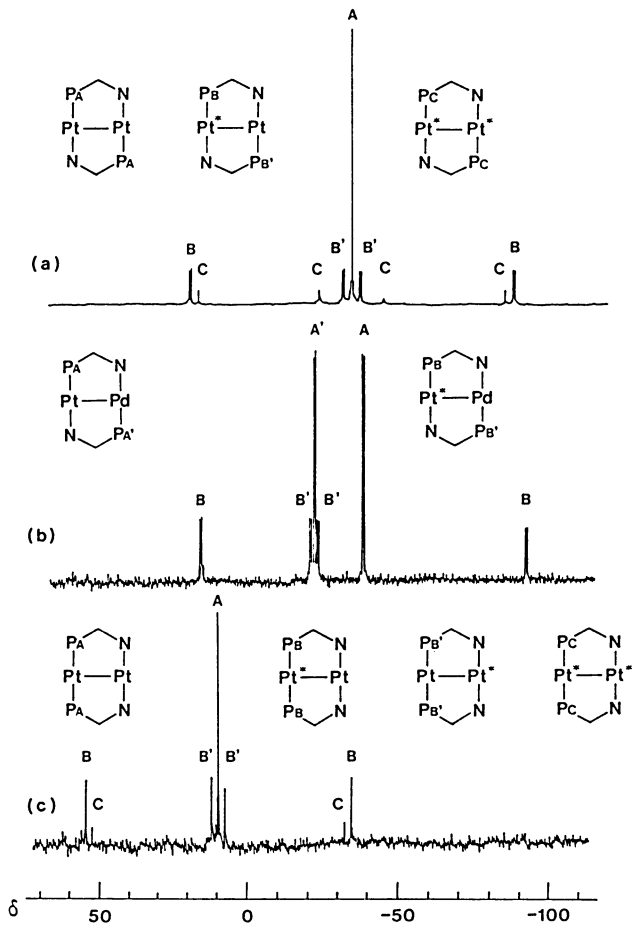

Fig. 2. $^{31}P\{^1H\}$ NMR spectra of *HT*-$[Pt_2Cl_2(\mu\text{-}Me_2Ppy)_2]$ (a), *HT*-$[PdPtCl_2(\mu\text{-}Me_2Ppy)_2]$ (b), and *HH*-$[Pt_2Br_2(\mu\text{-}Ph_2Ppy)_2]$ (c). A, A′, B, B′, and C correspond to the marked phosphorus atoms, and Pt* denotes ^{195}Pt.

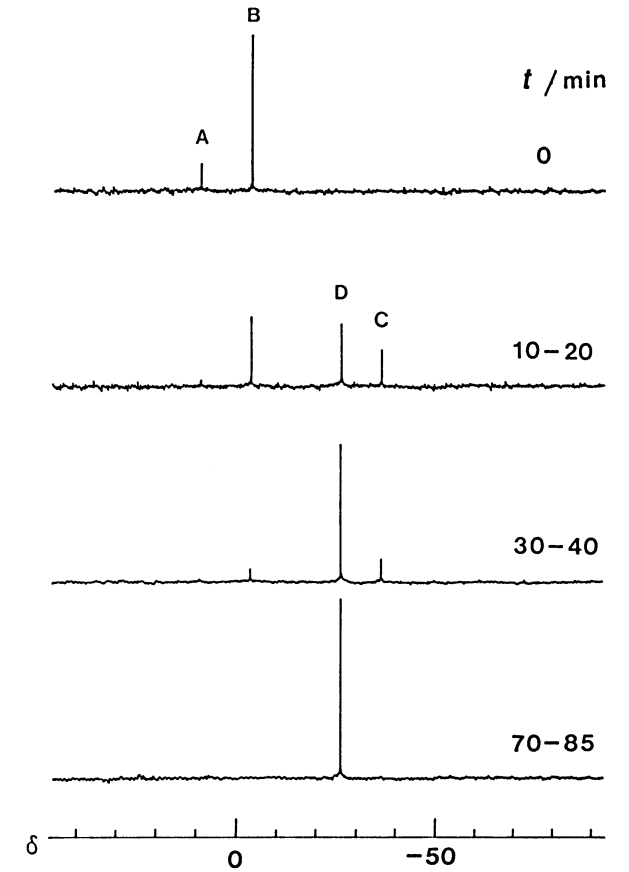

Fig. 4. $^{31}P\{^1H\}$ NMR spectral changes in the reaction between $[PdBr_2(Me_2Ppy\text{-}P)_2]$ and $[Pd_2(dba)_3]$. A, B, C, and D correspond to *cis*-$[PdBr_2(Me_2Ppy\text{-}P)_2]$, *trans*-$[PdBr_2(Me_2Ppy\text{-}P)_2]$, *HH*-$[Pd_2Br_2(\mu\text{-}Me_2Ppy)_2]$, and *HT*-$[Pd_2Br_2(\mu\text{-}Me_2Ppy)_2]$, respectively.

Table 3. ^{1}H and $^{13}C\{^{1}H\}$ NMR Data of *HT*-$[M_2X_2(\mu\text{-}Me_2Ppy)_2]$ (M_2=Pd_2, Pt_2, and PdPt)[a]

Complex	^{1}H		$^{13}C\{^{1}H\}$					
	Pd–P–C<u>H</u>$_3$	Pt–P–C<u>H</u>$_3$	P-<u>C</u>H$_3$	py-3	py-5	py-4	py-6	py-2
(Me_2Ppy)	1.26 (d: 2.6)		13.10 (d: 13.1)	125.36 (d: 24.2)	121.44 (s)	134.93 (d: 4.8)	149.66 (d: 6.2)	167.91 (d: 4.1)
HT-$[Pd_2Cl_2(\mu\text{-}Me_2Ppy)_2]$	2.09 (vt: ca. 10.6)		17.49 (v5)	124.76 (t: 5.5)	125.77 (s)	137.91 (t: 2.8)	152.51 (t: 6.2)	170.48 (v4)
HT-$[Pd_2Br_2(\mu\text{-}Me_2Ppy)_2]$	2.16 (vt: ca. 10.3)		18.93 (v5)	124.89 (t: 5.5)	125.86 (s)	137.66 (t: 2.8)	153.73 (t: 6.2)	170.50 (v4)
HT-$[Pd_2I_2(\mu\text{-}Me_2Ppy)_2]$	2.28 (vt: ca. 10.1)		21.60 (v5)	125.14 (t: 5.2)	125.88 (s)	137.16 (t: 2.1)	155.88 (t: 6.2)	170.86 (v4)
HT-$[Pt_2Cl_2(\mu\text{-}Me_2Ppy)_2]$		2.15 (vt: ca. 11.2) [44.4]	16.14 (m)	125.78 (t: 7.3)	126.33 (s)	137.64 (t: 2.8)	152.31 (t: 4.8)	
HT-$[Pt_2Br_2(\mu\text{-}Me_2Ppy)_2]$		2.21 (vt: ca. 11.0) [44.6]	17.58 (m)	125.94 (m)	126.58 (s)	137.37 (m)	154.02 (t: 4.8)	
HT-$[Pt_2I_2(\mu\text{-}Me_2Ppy)_2]$		2.36 (vt: ca. 10.8) [45.5]	20.03 (m)	126.29 (m)	126.62 (s)	136.81 (t: 2.8)	156.29 (t: 4.8)	
HT-$[PdPtCl_2(\mu\text{-}Me_2Ppy)_2]$	2.10 (vt: ca. 10.5) [7.0]	2.15 (vt: ca. 11.0) [43.5]						
HT-$[PdPtBr_2(\mu\text{-}Me_2Ppy)_2]$	2.17 (vt: ca. 10.5) [7.0]	2.22 (vt: ca. 11.0) [44.0]						
HT-$[PdPtI_2(\mu\text{-}Me_2Ppy)_2]$	2.27 (vt: ca. 10.1) [—]	2.34 (vt: ca. 10.8) [45.4]						

a) s, d, t, m, vt, v4, and v5 denote singlet, doublet, triplet, multiplet, virtual triplet, virtual quartet, and virtual quintet, respectively. Coupling constants to ^{31}P and ^{195}Pt are written in ( ) and [ ], respectively, in Hz.

tively.[8] Thus $[Pd_2Br_2(\mu\text{-}Me_2Ppy)_2]$ can be assigned to the *HT*-isomer. The corresponding dichloro and diiodo complexes were similarly assigned as the *HT*-isomer. For $[Pd_2X_2(\mu\text{-}Ph_2Ppy)_2]$, NMR spectra provide no useful information for assigning the structure. However, the ^{31}P signals of these complexes are observed in the region expected from the ^{31}P chemical shifts of the *HT*-isomers of Pt(I)–Pt(I) and Pd(I)–Pt(I) complexes of Ph_2Ppy (Table 2). Furthermore, the patterns of absorption spectra are similar to those of *HT*-$[Pd_2X_2(\mu\text{-}Me_2Ppy)_2]$ (vide infra). Thus all of $[Pd_2X_2(\mu\text{-}Ph_2Ppy)_2]$ (X=Cl, Br, and I) were assigned to the *HT*-isomer. The structures of *HT*-$[Pd_2Cl_2(\mu\text{-}Me_2Ppy)_2]$, *HT*-$[Pt_2Cl_2(\mu\text{-}Me_2Ppy)_2]$, *HT*-$[PdPtCl_2(\mu\text{-}Me_2Ppy)_2]$, and *HT*-$[Pd_2Cl_2(\mu\text{-}Ph_2Ppy)_2]$ have been confirmed by X-ray analyses.[15]

Except *HH*-$[Pt_2I_2(\mu\text{-}Ph_2Ppy)_2]$ and *HH*-$[Pt_2Br_2(\mu\text{-}Ph_2Ppy)_2]$, all the dinuclear complexes obtained by reaction (1) have the *HT* structure. Farr, Wood, and Balch[7] reported that the reaction between $[PtI_2(Ph_2Ppy\text{-}P)_2]$ and $[Pt_2(dba)_3]$ afforded only *HH*-isomer, and the *HT*-isomer was obtained by axial-ligand substitution of *HT*-$[Pt_2Cl_2(\mu\text{-}Ph_2Ppy)_2]$ with KI. However, both *HH*- and *HT*-isomers of $[Pt_2Br_2(\mu\text{-}Ph_2Ppy)_2]$ were formed in similar amounts by the reaction of $[PtBr_2(Ph_2Ppy\text{-}P)_2]$ with $[Pt_2(dba)_3]$. The isomers could be separated by solubility difference in dichloromethane.

All of the dinuclear complexes obtained in this study are stable in the solid state, but the bromo and iodo complexes of Pd(I)–Pd(I) and Pd(I)–Pt(I) in solution decompose slowly to give a black precipitate. The Pd(I) and Me_2Ppy complexes seem to be less stable than the Pt(I) and Ph_2Ppy complexes, respectively.

Conproportionation Reactions. To examine reaction (1) in more detail, reactions between $[MX_2(R_2Ppy\text{-}P)_2]$ (0.05—0.1 mmol) and a stoichiometric amount of $[M_2(dba)_3]$ in $CDCl_3$ (ca. 1.5 cm^3) were followed by $^{31}P\{^{1}H\}$ NMR spectra at 33 °C.

Figure 4 shows the spectral changes in the reaction between $[PdBr_2(Me_2Ppy\text{-}P)_2]$ with $[Pd_2(dba)_3]$. The spectra exhibit peaks for the reactant (δ=10.98; cis and 0.73; trans), the final product (δ=−25.83; *HT*-isomer), and an intermidiate (δ=−36.29) which can be assigned as the *HH*-isomer on the basis of spectral changes in the reactions of the Ph_2Ppy complexes described later. Similar spectral changes were observed in the reactions of the corresponding iodo and chloro complexes (Table 2). Rates of the reactions were larger in the order of the iodo>bromo>chloro complexes, and the reactions were completed in 30, 70, and 90 min, respectively. The reactions of $[PtX_2(Me_2Ppy\text{-}P)_2]$ (X=Cl and Br) and $[Pt_2(dba)_3]$ proceeded much slower than those of the palladium complexes. After 3 d, 20 and 65% of the chloro and bromo complexes reacted, respectively, with

$[Pt_2(dba)_3]$. The spectra showed only peaks for the reactant and the final product (*HT*-isomer), no peak due to the *HH*-isomer being detected. The reaction between $[PtI_2(Me_2Ppy\text{-}P)_2]$ and $[Pt_2(dba)_3]$ showed spectral changes different from those of the above reactions as shown in Fig. 5. The starting $[PtI_2(Me_2Ppy\text{-}P)_2]$ complex disappeared within 1 h, and *HH*-$[Pt_2I_2(\mu\text{-}Me_2Ppy)_2]$, which was assigned on the basis of the spectral pattern and coupling constants, was formed. This *HH*-isomer isomerized slowly to the *HT*-isomer. After 5 d, the formation ratio of the *HH*- to the *HT*-isomers was evaluated as ca. 1 : 2 from the peak height. Isolation of the crystalline *HH*-isomer was unsuccessful because of isomerization to the *HT*-isomer during the crystallization.

The reactions of $[PdX_2(Ph_2Ppy\text{-}P)_2]$ (X=Cl, Br, and I) with $[Pd_2(dba)_3]$ were similar to the above $[Pd_2X_2(\mu\text{-}Me_2Ppy)_2]$ (Fig. 6). A resonance assignable to the unstable *HH*-isomer was observed at $\delta=-12.44$ (X=Cl), -14.31 (X=Br), and -16.66 (X=I). The reactant diminished rapidly, while the isomerization of the *HH*- to the *HT*-isomer was rather slow compared to the Me_2Ppy complexes. However, the isomerization was not so slow as to be isolable the *HH*-isomer. The reactions of $[PtX_2(Ph_2Ppy\text{-}P)_2]$ (X=Cl and Br) with $[Pt_2(dba)_3]$ were similar to those of the corresponding Pd(I) complexes, but proceeded more slowly to yield the *HH*-isomer which slowly isomerized to the *HT*-isomer. The isomerization of the chloro complex was completed in 2 d, while the bromo complex was a 1 : 1 mixture of the *HH*- and *HT*-isomers even after 3 d. Thus *HH*-$[Pt_2Br_2(\mu\text{-}Ph_2Ppy)_2]$ was isolated as crystals. The reaction between $[PtI_2(Ph_2Ppy\text{-}P)_2]$ and $[Pt_2(dba)_3]$ produced only *HH*-$[Pt_2I_2(\mu\text{-}Ph_2Ppy)_2]$ as reported by Farr, Wood, and Balch.[7] No isomerization of the *HH*-isomer was observed under the experimental conditions. The stability of *HH*-$[Pt_2X_2(\mu\text{-}Ph_2Ppy)_2]$ depends largely on the kind of X.

The starting Pd(II) and Pt(II) complexes in $CDCl_3$ at 33 °C exist as a *cis*-isomer ($[PtX_2(R_2Ppy\text{-}P)_2]$ (X=Cl, Br; R=Me, and Ph), a *trans*-isomer ($[PdI_2(Me_2Ppy\text{-}P)_2]$ and $[PdX_2(Ph_2Ppy\text{-}P)_2]$ (X=Br and I)), or a *cis-trans* equilibrium mixture ($[PdX_2(Me_2Ppy\text{-}P)_2]$ (X=Cl and Br), $[PdCl_2(Ph_2Ppy\text{-}P)_2]$, and $[PtI_2(R_2Ppy\text{-}P)_2]$ (R=Me and Ph)).[7,9,14] From $^{31}P\{^1H\}$ NMR studies, however, the reactions of these complexes with $[M_2(dba)_3]$ seem to proceed by a similar pathway; dimerization yielding

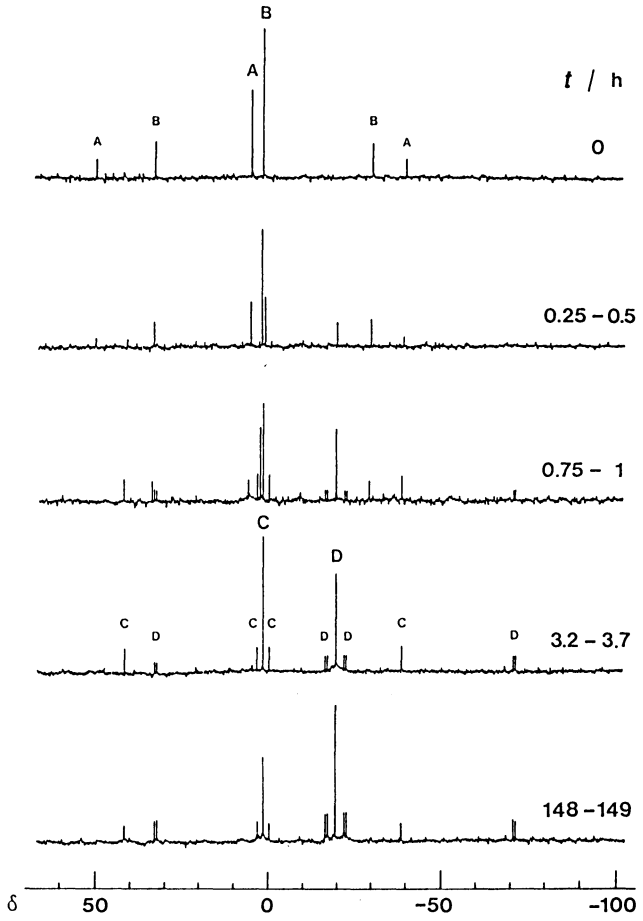

Fig. 5. $^{31}P\{^1H\}$ NMR spectral changes in the reaction between $[PtI_2(Me_2Ppy\text{-}P)_2]$ and $[Pt_2(dba)_3]$. A, B, C, and D correspond to *cis*-$[PtI_2(Me_2Ppy\text{-}P)_2]$, *trans*-$[PtI_2(Me_2Ppy\text{-}P)_2]$, *HH*-$[Pt_2I_2(\mu\text{-}Me_2Ppy)_2]$, and *HT*-$[Pt_2I_2(\mu\text{-}Me_2Ppy)_2]$, respectively.

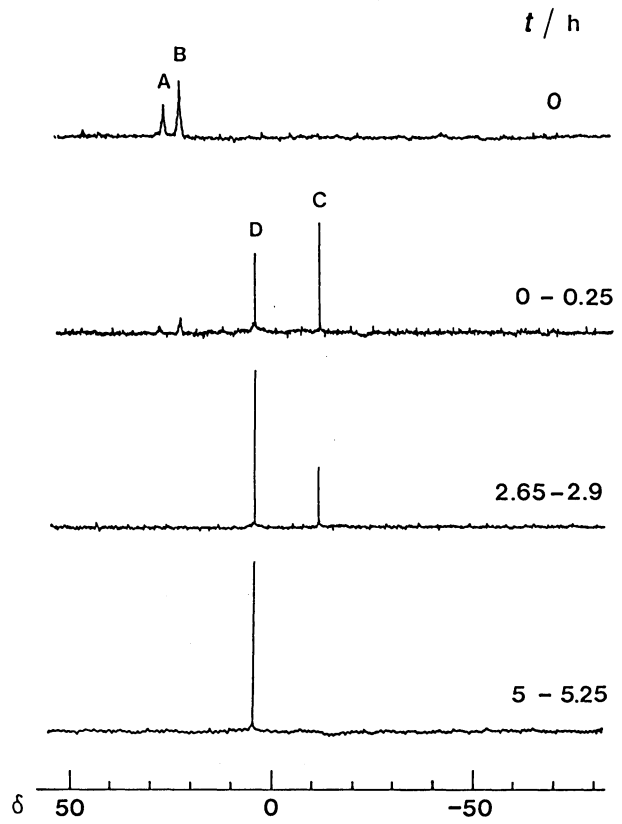

Fig. 6. $^{31}P\{^1H\}$ NMR spectral changes in the reaction between $[PdCl_2(Ph_2Ppy\text{-}P)_2]$ and $[Pd_2(dba)_3]$. A, B, C, and D correspond to *cis*-$[PdCl_2(Ph_2Ppy\text{-}P)_2]$, *trans*-$[PdCl_2(Ph_2Ppy\text{-}P)_2]$, *HH*-$[Pd_2Cl_2(\mu\text{-}Ph_2Ppy)_2]$, and *HT*-$[Pd_2Cl_2(\mu\text{-}Ph_2Ppy)_2]$, respectively.

the *HH*-isomer and then its isomerization to the *HT*-isomer, although signals due to the *HH*-isomer were not detected for $[Pt_2X_2(\mu\text{-}Me_2Ppy)_2]$ (X=Cl and Br). The absence of signals for *HH*-$[Pt_2X_2(\mu\text{-}Me_2Ppy)_2]$ (X=Cl and Br) might be attributable to slow dimerization and rapid isomerization to the *HT*-isomer. The Me_2Ppy ligand is more basic than Ph_2Ppy and might exert a strong trans effect on a metal ion, so that the *HH*-isomer, where two phosphorous donor atoms are at the *trans* coordination positions of one metal ion, will be unstable and isomerize rapidly to the stable *HT*-isomer. For the formation of the *HH*-isomer by dimerization, the *trans*-isomer of starting $[MX_2(R_2Ppy\text{-}P)_2]$ would be more favorable than the *cis*-isomer, since two phosphine ligands can retain their coordination positions. However, it is unknown which isomer is more reactive. The complex which exists as a *cis–trans* equilibrium mixture did not change the equilibrium ratio of the isomers during the reaction.

The Pd(II) complexes react more rapidly than do the corresponding Pt(II) complexes in both dimerization and isomerization. Rates of these reactions are changed by the kind of X, although the changes are not so clear. For each halogeno series of the complexes, it seems that the dimerization occurs faster in the order of Cl<Br<I, while the order in the isomerization is reversed, Cl>Br>I. We have no appropriate explanation for these reactivity differences at present.

For the heteronuclear Pd(I)–Pt(I) complexes, there are two preparative methods;

(a) $[Pt^{II}X_2(R_2Ppy\text{-}P)_2] + 1/2\,[Pd^0{}_2(dba)_3]$

(b) $[Pd^{II}X_2(R_2Ppy\text{-}P)_2] + 1/2\,[Pt^0{}_2(dba)_3]$

$\rightarrow [PdPtX_2(\mu\text{-}R_2Ppy)_2]$.

In this study both (a) and (b) reactions for $[PdPtI_2(\mu\text{-}Me_2Ppy)_2]$ were followed similarly by $^{31}P\{^1H\}$ NMR spectra (Fig. 7). In reaction (a), *HH(PPt)*-$[PdPtI_2(\mu\text{-}Me_2Ppy)_2]$ was formed soon after the reaction had started, and then slowly isomerized to the *HT*-isomer. After several hours, the spectrum showed only peaks for the *HT*-isomer and the unreacted starting Pt(II) complex. The Pt(II) complex also remained in reaction (a) using a slight excess of $[Pd_2(dba)_3]$. In the presence of $[PtI_2(Me_2Ppy\text{-}P)_2]$, $[Pd_2(dba)_3]$ seems to decompose easily. After the reaction, a black material, probably metallic Pd adhered to the reaction vessel. A certain reaction would take place between $[PtI_2(Me_2Ppy\text{-}P)_2]$ and $[Pd_2(dba)_3]$ to yield inactive Pd species, and the Pt(II) complex remains unreacted. *HT*-$[PdPtI_2(\mu\text{-}Me_2Ppy)_2]$ was isolated as crystals from the product of reaction (a) by recrystallization.

In reaction (b), *HT*-$[PdPtI_2(\mu\text{-}Me_2Ppy)_2]$ and *HT*-$[Pd_2I_2(\mu\text{-}Me_2Ppy)_2]$ were slowly formed in similar rates,

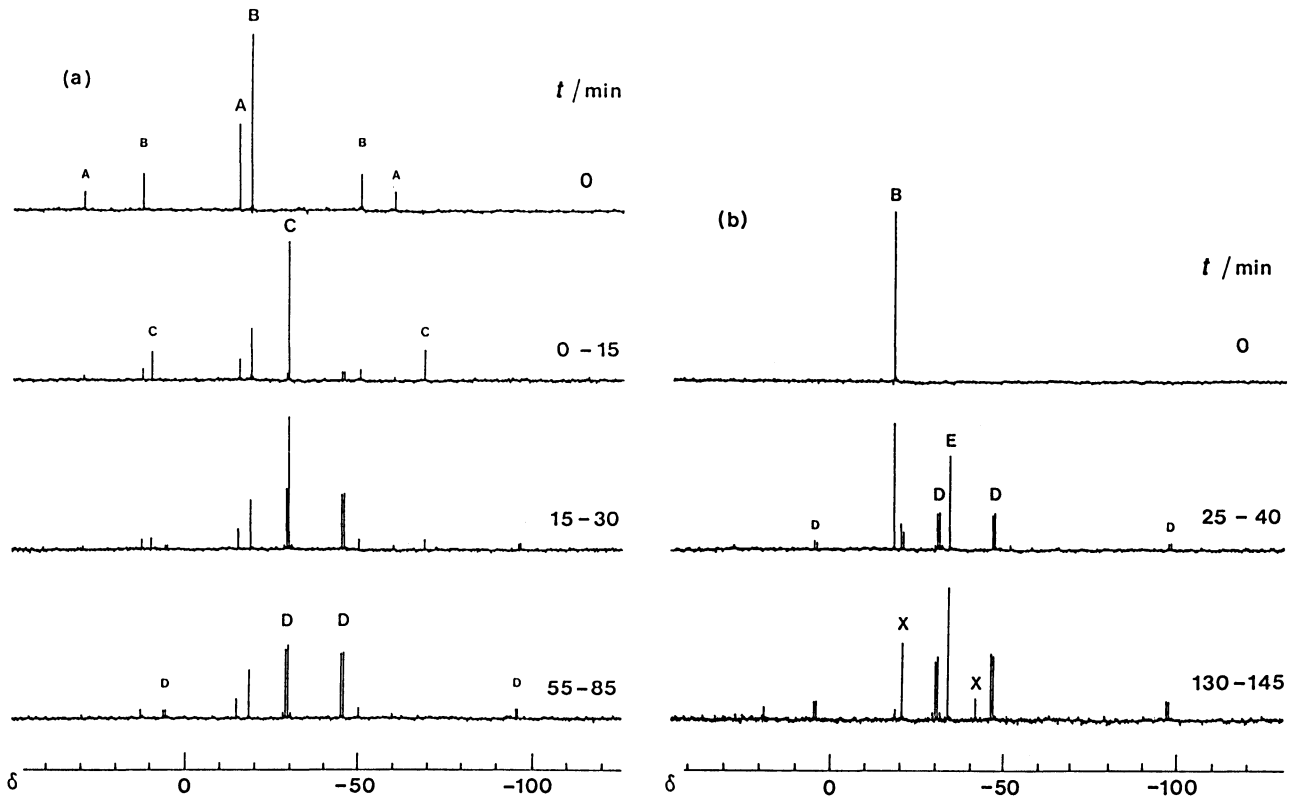

Fig. 7. $^{31}P\{^1H\}$ NMR spectral changes in the reactions between $[PtI_2(Me_2Ppy\text{-}P)_2]$ and $[Pd_2(dba)_3]$ (a) and between $[PdI_2(Me_2Ppy\text{-}P)_2]$ and $[Pt_2(dba)_3]$ (b). A, B, C, D, E, and X correspond to *cis*-$[M^{II}I_2(Me_2Ppy\text{-}P)_2]$, *trans*-$[M^{II}I_2(Me_2Ppy\text{-}P)_2]$ (M=Pt for (a) and Pd for (b)), *HH(PPt)*-$[PdPtI_2(\mu\text{-}Me_2Ppy)_2]$, *HT*-$[PdPtI_2(\mu\text{-}Me_2Ppy)_2]$, *HT*-$[Pd_2I_2(\mu\text{-}Me_2Ppy)_2]$, and unassignable species, respectively.

but formation of *HH*-[$PdPtI_2(\mu$-$Me_2Ppy)_2$] was not observed. The spectra showed several unassignable species. These by-products were not removed from *HT*-[$PdPtI_2(\mu$-$Me_2Ppy)_2$] by chromatograpy or recrystallization. The starting Pd(II) complex will be less stable than the Pt(II) complex, and might decompose partly in the process of dimerization by a redox reaction with [$Pt_2(dba)_3$]. Thus reaction (a) is more advantageous than reaction (b) for the preparation of heterodinuclear complexes.

Electronic Spectra. Table 4 lists absorption spectral data of the dinuclear complexes prepared in this study, together with those reported for the related complexes. In Fig. 8 are shown the spectra of two series, *HT*-[$Pt_2X_2(\mu$-$Me_2Ppy)_2$] (a) and *HT*-[$Pd_2X_2(\mu$-$Me_2Ppy)_2$] (b) (X=Cl, Br, and I). For each series, the spectral patterns are similar to one another, and each band is shifted to lower energy as X proceeds from Cl through Br to I. The band intensities increase also in the same order except the bands around 30000 cm^{-1} in *HT*-[$Pd_2X_2(\mu$-$Me_2Ppy)_2$]. Similar spectral patterns and features have been observed for the analogous dinuclear Pd(I) and Pt(I) series complexes bridged by diphosphine ligands as listed in Table 4.[2,8,16,17] For these dinuclear complexes with a fairly strong metal–metal bond as revealed by X-ray analysis,[8,15,17,18] no plausible band assignment can be given at present. Alves, Vitorge, and Sourisseau[16] reported the spectra of [(Pd or $Pt)_2X_2(\mu$-$dppm)_2$], the patterns of which are similar to those of the Me_2Ppy complexes, and attributed three major bands around 24000, 29000, and 33000 cm^{-1} to three d–d transitions arising from the $(\sigma)^2(\pi)^4(\delta)^4$-$(\delta^*)^4(\pi^*)^4(\sigma^*)^0$ configuration of 18e transition metal dimers. In their assignment, the Pd complex has all the bands at higher energies than those of the corresponding bands of the Pt complex. From a comparison of the spectra of Pd and Pt complexes in Fig. 8, however, the three bands around 20000, 26000, and 32000 cm^{-1} of the Pt complex seem to correspond to a shoulder around 18000 cm^{-1}, and two strong bands around 21000 and 29000 cm^{-1} of the Pd complex, respectively. Figure 9(a) compares the spectra of *HT*-[(Pd_2, PdPt, or Pt_2)Cl_2-$(\mu$-$Me_2Ppy)_2$]. The PdPt complex shows a nearly average spectrum between those of the Pd_2 and Pt_2 complexes in the two lower energy transition region, although the spectrum in the higher energy region is not

Table 4. Absorption Spectral Data of the Dinuclear Complexes[a]

Complex	$\sigma_{max}/10^3$ cm^{-1} ($\log(\varepsilon/mol^{-1}\,dm^3\,cm^{-1})$)				
HT-[$Pd_2Cl_2(\mu$-$Me_2Ppy)_2$]	18.5[sh](ca. 2.3)	22.42(3.74)		31.41(4.09)	38.5[sh](4.28)
HT-[$Pd_2Br_2(\mu$-$Me_2Ppy)_2$]	18.2[sh](ca. 2.5)	21.81(3.87)		29.85(4.15)	38.8[sh](4.30)
HT-[$Pd_2I_2(\mu$-$Me_2Ppy)_2$]	17.6[sh](ca. 3.4)	20.28(4.02)		27.13(4.09)	
HT-[$PdPtCl_2(\mu$-$Me_2Ppy)_2$]	20.8[sh](ca. 2.5)	24.68(3.49)	30.8[sh](3.83)	34.8[sh](4.15)	39.2[sh](4.38)
HT-[$PdPtBr_2(\mu$-$Me_2Ppy)_2$]	20.5[sh](ca. 2.7)	24.15(3.61)		33.57(4.20)	38.8[sh](4.34)
HT-[$PdPtI_2(\mu$-$Me_2Ppy)_2$]	20.1[sh](ca. 3.2)	22.73(3.81)	30.5[sh](4.15)	31.63(4.17)	38.8[sh](4.35)
HT-[$Pt_2Cl_2(\mu$-$Me_2Ppy)_2$]	21.17(2.38)	26.82(3.50)	32.22(3.83)		40.96(4.53)
HT-[$Pt_2Br_2(\mu$-$Me_2Ppy)_2$]	20.76(2.50)	26.44(3.57)	32.1[sh](3.90)	37.6[sh](4.45)	39.56(4.53)
HT-[$Pt_2I_2(\mu$-$Me_2Ppy)_2$]	19.93(2.82)	25.81(3.78)	32.1[sh](4.38)	34.53(4.43)	38.82(4.43)
HT-[$Pd_2Cl_2(\mu$-$Ph_2Ppy)_2$]	ca. 18[sh](ca. 2.5)	21.42(3.83)		29.93(4.10)	37.2[sh](4.43)
HT-[$Pd_2Br_2(\mu$-$Ph_2Ppy)_2$]	ca. 17[sh](ca. 2.8)	20.58(3.94)	26.1[sh](3.69)	28.57(4.15)	36.0[sh](4.34)
HT-[$Pd_2I_2(\mu$-$Ph_2Ppy)_2$]	ca. 16[sh](ca. 3.2)	18.48(3.97)	23.8[sh](3.80)	26.33(4.06)	35.6[sh](4.35)
HT-[$PdPtCl_2(\mu$-$Ph_2Ppy)_2$]	20.0[sh](2.60)	24.00(3.61)		33.60(4.22)	
HT-[$PdPtBr_2(\mu$-$Ph_2Ppy)_2$]	19.4[sh](2.80)	23.18(3.78)		32.02(4.28)	
HT-[$PdPtI_2(\mu$-$Ph_2Ppy)_2$]	17.9[sh](3.10)	21.12(3.94)		29.15(4.22)	37.8[sh](4.58)
HT-[$Pt_2Cl_2(\mu$-$Ph_2Ppy)_2$]	20.35(2.38)	26.11(3.51)	31.1[sh](3.92)		38.0[sh](4.50)
HT-[$Pt_2Br_2(\mu$-$Ph_2Ppy)_2$]	20.14(2.54)	25.85(3.64)	30.3[sh](3.96)	32.8[sh](4.21)	37.1[sh](4.48)
HT-[$Pt_2I_2(\mu$-$Ph_2Ppy)_2$]	18.6[sh](2.86)	24.92(3.80)		31.0(4.34)	37.9[sh](4.58)
HH-[$Pt_2Br_2(\mu$-$Ph_2Ppy)_2$]	21.1(2.43)	25.7[sh](3.50)	29.3[sh](4.00)	34.0[sh](4.36)	38.8[sh](4.67)
HH-[$Pt_2I_2(\mu$-$Ph_2Ppy)_2$]	19.93(2.66)	23.7[sh](3.59)		31.5[sh](4.39)	
[$Pd_2Cl_2(\mu$-dmpm)$_2$][b]		25.97(3.76)	31.25(4.12)	35.97(4.34)	
[$Pd_2Br_2(\mu$-dmpm)$_2$][b]		25.38(3.98)	30.03(4.34)	35.84(4.33)	
[$Pd_2Cl_2(\mu$-dppm)$_2$][c]		24.04(3.88)	28.82(4.23)	34.13(4.41)	
[$Pd_2Br_2(\mu$-dppm)$_2$][c]		23.36(4.03)	27.47(4.24)	33.22(4.36)	
[$Pd_2I_2(\mu$-dppm)$_2$][c]		20.49(4.11)			
		23.31(4.08)	25.38(4.08)	31.95(4.30)	
[$Pt_2Cl_2(\mu$-dppm)$_2$][d]	23.64(2.30)	28.01(3.41)	31.25(3.89)		
[$Pd_2Cl_2(\mu$-Medppm)$_2$][e]		24.88(3.97)	29.24(4.32)	34.25(4.48)	
[$Pd_2Br_2(\mu$-Medppm)$_2$][e]		24.10(4.08)	27.78(4.30)	33.33(4.38)	
[$Pd_2I_2(\mu$-Medppm)$_2$][e]	17.70(3.61)	20.75(4.13)			
		23.15(4.17)	25.32(4.18)	31.95(4.36)	
[$Pd_2Cl_2(\mu$-Medppm)(μ-Ph_2Ppy)][e]		23.26(3.80)	29.07(4.08)	36.1[sh](4.37)	
[$Pd_2Cl_2(\mu$-Medppm)(μ-dppm)][e]		24.39(3.91)	29.24(4.25)	34.36(4.44)	

a) sh denotes shoulder absorption. b), c), d), and e) are data taken from references 17, 2, 16, and 8, respectively.

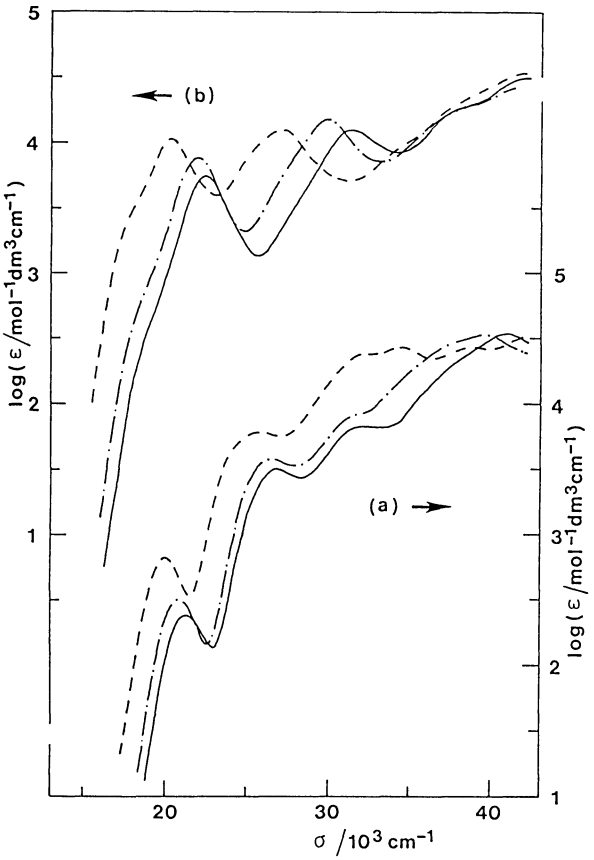

Fig. 8. Electronic spectra of *HT*-[$Pt_2X_2(\mu\text{-}Me_2Ppy)_2$] (a) and *HT*-[$Pd_2X_2(\mu\text{-}Me_2Ppy)_2$] (b) (X=Cl (——), Br (— · —), and I (----)) in dichloromethane.

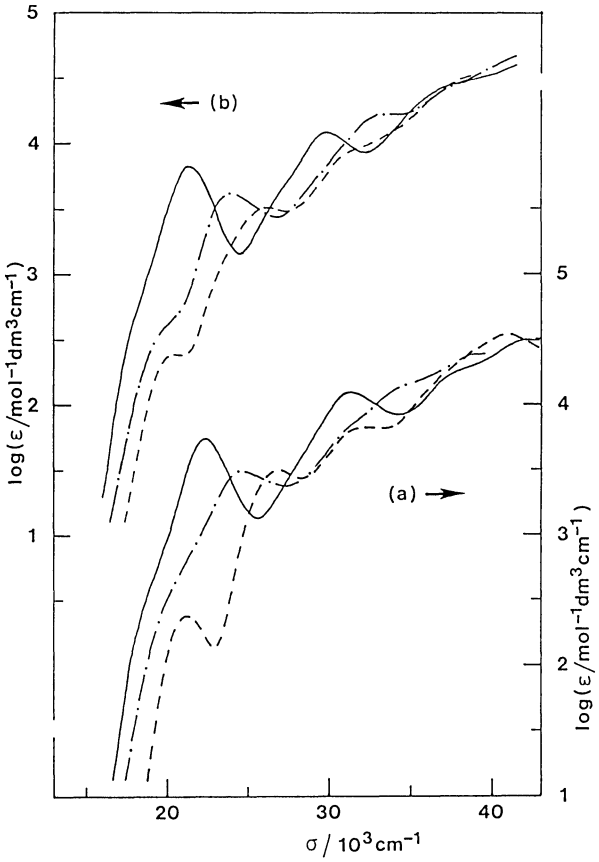

Fig. 9. Electronic spectra of *HT*-[$M_2Cl_2(\mu\text{-}Me_2Ppy)_2$] (a) and *HT*-[$M_2Cl_2(\mu\text{-}Ph_2Ppy)_2$] (b) ($M_2$=$Pd_2$ (——), PdPt (— · —), and Pt_2 (----)) in dichloromethane.

clear. This spectral relation among the Pd_2, PdPt, and Pt_2 complexes may support the conclusion that the shoulder absorption around 18000 cm^{-1} of *HT*-[$Pd_2X_2(\mu\text{-}Me_2Ppy)_2$] corresponds to the lowest energy band of the corresponding Pt complex.

Figure 9(b) and Table 4 show that the Ph_2Ppy complexes exhibit very similar spectra to those of the Me_2Ppy complexes, but all the bands of the Ph_2Ppy complexes are observed at lower energy by 1000—1500 cm^{-1} than the corresponding bands of the Me_2Ppy complexes. The energy differences in band maxima between the analogous dppm[2] and dmpm ($(CH_3)_2PCH_2P(CH_3)_2$)[17] complexes are 2000—2500 cm^{-1}, the bands of dppm complexes being at lower energy. Including the spectral data of [$Pd_2X_2(\mu\text{-}Medppm)_2$],[8] the bands of [$Pd_2X_2(\mu\text{-}L)_2$] are shifted to higher energy in the order of L=Ph_2Ppy<Me_2Ppy<dppm< Medppm<dmpm. This sequence is the one expected from the spectrochemical series.

Figure 10 compares the spectra of *HT*- and *HH*-[$Pt_2Br_2(\mu\text{-}Ph_2Ppy)_2$]. The *HH*-isomer shows the lowest energy band at higher energy, the second band at nearly the same energy, and the third band at lower energy compared, respectively, with the corresponding bands of the *HT*-isomer. A similar spectral relation is seen between the *HT*- and *HH*-isomers of the diiodo com-

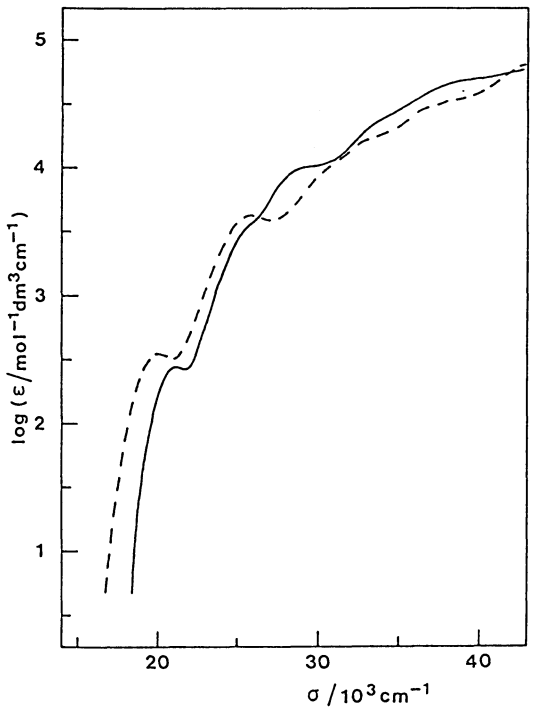

Fig. 10. Electronic spectra of *HH*-[$Pt_2Br_2(\mu\text{-}Ph_2Ppy)_2$] (——) and *HT*-[$Pt_2Br_2(\mu\text{-}Ph_2Ppy)_2$] (----) in dichloromethane.

plex. Such a spectral difference arising from the different configuration of donor groups would provide useful information to elucidate electronic states of dinuclear complexes. However, we have no explanation for this difference at present.

This work was supported by a Grant-in-Aid for Scientific Research No. 03453047 from the Ministry of Education, Science and Culture.

References

1) "Conprehensive Coordination Chemlstry," ed by G. Wilkinson, P. D. Gillard, and J. A. McCleverty, Pergamon Press, Vol. 5, pp. 456—462 and pp. 1103—1110.

2) L. S. Benner and A. L. Balch, *J. Am. Chem. Soc.*, **100**, 6099 (1978).

3) M. P. Brown, R. J. Puddephatt, M. Rashidi, and K. R. Seddon, *J. Chem. Soc., Dalton Trans.*, **1977**, 951.

4) P. G. Pringle and B. L. Shaw, *J. Chem. Soc., Dalton Trans.*, **1983**, 889.

5) R. R. Guimerans and A. L. Balch, *Inorg. Chim. Acta,* **77**, L177 (1983); G. K. Anderson and R. Kumar, *J. Organomet. Chem.*, **342**, 263 (1988); Y. Fuchita, K. I. Hardcastle, K. Hiraki, and M. Kawatani, *Bull. Chem. Soc. Jpn.*, **63**, 1961 (1990).

6) A. Maisonnat, J. P. Farr, and A. L. Balch, *Inorg. Chim. Acta,* **53**, L217 (1981).

7) J. P. Farr, F. E. Wood, and A. L. Balch, *Inorg. Chem.*, **22**, 3387 (1983).

8) C.-L. Lee, Y.-P. Yang, S. J. Rettig, B. R. James, D. A. Nelson, and M. A. Lilga, *Organometallics,* **5**, 2220 (1986).

9) T. Suzuki, M. Kita, K. Kashiwabara, and J. Fujita, *Bull. Chem. Soc. Jpn.*, **63**, 3434 (1990).

10) Y. Inoguchi, B. Milewski-Mahrla, and H. Schmidbaur, *Chem. Ber.*, **115**, 3085 (1983).

11) J. P. Farr, M. M. Olmstead, F. E. Wood, and A. L. Balch, *J. Am. Chem. Soc.*, **105**, 792 (1983).

12) T. Ukai, H. kawazura, Y. Ishii, J. J. Bonnet, and J. A. Ibers, *J. Organomet. Chem.*, **65**, 253 (1974).

13) H. Tanaka and H. Kawazura, *Bull. Chem. Soc. Jpn.*, **52**, 2815 (1979).

14) A. Maisonnet, J. P. Farr, M. M. Olmstead, C. T. Hunt, and A. L. Balch, *Inorg. Chem.*, **21**, 3961 (1982).

15) T. Suzuki et al., to be published.

16) O. L. Alves, M.-C. Vitorge, and C. Sourisseau, *Nouv. J. Chim.*, **7**, 231 (1983).

17) M. L. Kullberg, F. R. Lemke, D. R. Powell, and C. P. Kubiak, *Inorg. Chem.*, **24**, 3589 (1985).

18) R. G. Holloway, B. R. Penfold, R. Colton, and M. J. McCormick, *J. Chem. Soc., Chem. Commun.*, **1976**, 485; M. P. Brown, R. J. Puddephatt, M. Rashidi, Lj. Manojlović-Muir, K. W. Muir, T. Solomun, and K. R. Seddon, *Inorg. Chim. Acta,* **23**, L33 (1977).